Electronic Supplementary Material (ESI) for Physical Chemistry Chemical Physics.

Supplementary Information for

Factors that affect volume change during electrochemical cycling in cathode materials for lithium ion batteries

Ying Wang[1], Jiahua Liu[1], Taowen Chen[1], Weicheng Lin[1], Jiaxin Zheng[1,2,]*

[1]School of Advanced Materials, Peking University, Shenzhen Graduate School, Shenzhen 518055, People's Republic of China

[2]Fujian science & technology innovation laboratory for energy devices of China (21C-LAB), Ningde 352100, People's Republic of China

AUTHOR INFORMATION

Corresponding Author

* Jiaxin Zheng, E-mail: zhengjx@pkusz.edu.cn

Li/Ni exchange

$LiNiO_2$ with a perfect crystal structure is not favorable because Ni ions are easily located in the lithium layers during synthesis and delithiation. Fig. S1a shows the structure models for the multi-

lattice of $LiNiO_2$, $LiNiO_2$ with one pair of Li-Ni exchange ($\frac{1}{12}$ content), and $Li_{0.92}Ni_{1.08}O_2$ with one Ni in Li layer. Their volumes are shown in Figure S1b. Obviously, the volume of $Li_{0.92-x}Ni_{1.08}O_2$ is always larger than $Li_{1-x}NiO_2$ during the delithiation, which is consistent with previous studies[1, 2] because more Ni^{2+} ions can expand the Ni slabs (r(Ni2+)>r(Ni3+). However, the volume of antisite $Li_{1-x}NiO_2$ is not always larger than $Li_{1-x}NiO_2$ because the presence of Ni^{3+} ions in the Li slabs shrinks the Li interslabs while Li^+ ions in the Ni slabs also shrink the Ni interslabs. Another interesting point is that the volume shrinkages are retarded at x < 0.5 for both antisite models, which may be a strategy for researchers to improve the volume stability of LNO.

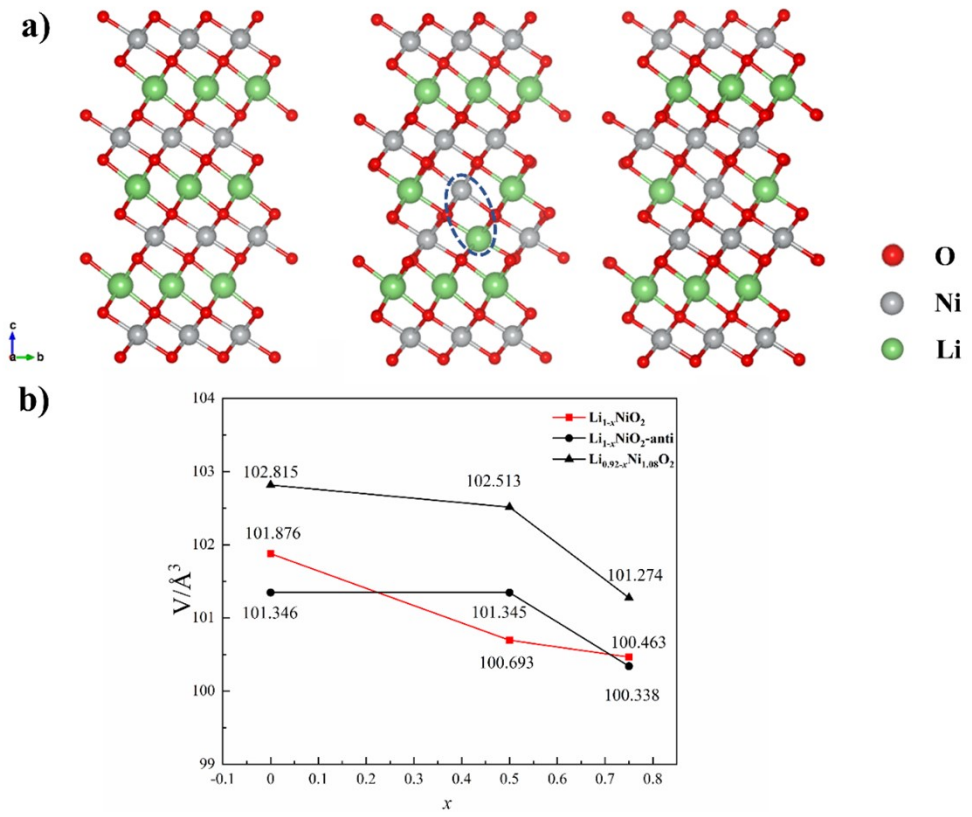

Figure S1. (a) Structure models for $LiNiO_2$ (left), $LiNiO_2$ with one pair of Li-Ni exchange ($\frac{1}{12}$ content) (middle), and $Li_{0.92}Ni_{1.08}O_2$ with one Ni in Li site (right); (b) their volumes in different lithium content.

Insertion Mechanisms

The practical insertion mechanisms of intercalation cathode materials are usually complex, and some are controversial until now, such as $LiFeBO_3$, whose first 0.5 Li are removed in a two-phase reaction, but the last 0.5 Li are removed from intermediate $Li_{0.5}FeBO_3$ phase through a solid solution mechanism[3]. The deintercalation mechanism of phosphate and most other polyanion family compounds is widely perceived as a two-phase separation mechanism (solid-solution reaction may occur to a specific and very narrow extent)[4-6]. We calculate the volumes of half-delithiated $LiFePO_4$, LiVPO4F, and $LiFeSO_4F$ in different insertion mechanisms (Figure S2, $1\times 1\times 8$ supercell). The difference between the volumes of cathodes materials in two deintercalation mechanisms are very tiny, especially for $LiVPO_4F$ and $LiFeSO_4F$, whose volume curves almost overlap, indicating the deintercalation mechanism may have little effort on volume change. Nevertheless, the conclusion needs further confirmation because the periodic condition of VASP makes it difficult to simulate the practical crystal particles taking part in two-phase reactions.

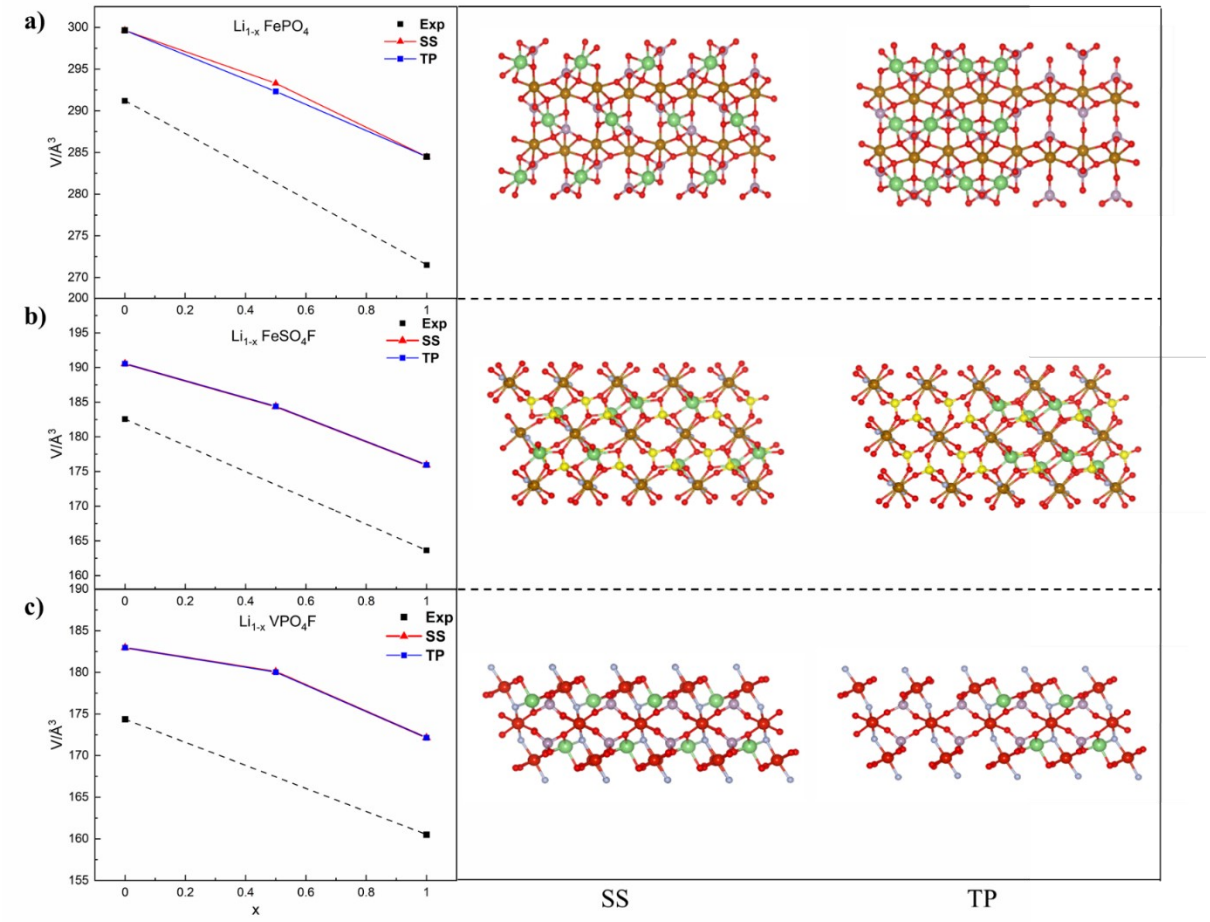

Figure S2. Volume curves and half delithiated crystal structures in solid-solution (SS) and two-phase (TP) delithiation mechanism of (a) $LiFePO_4$ (b) $LiFeSO_4F$ and (c) $LiVPO_4F$

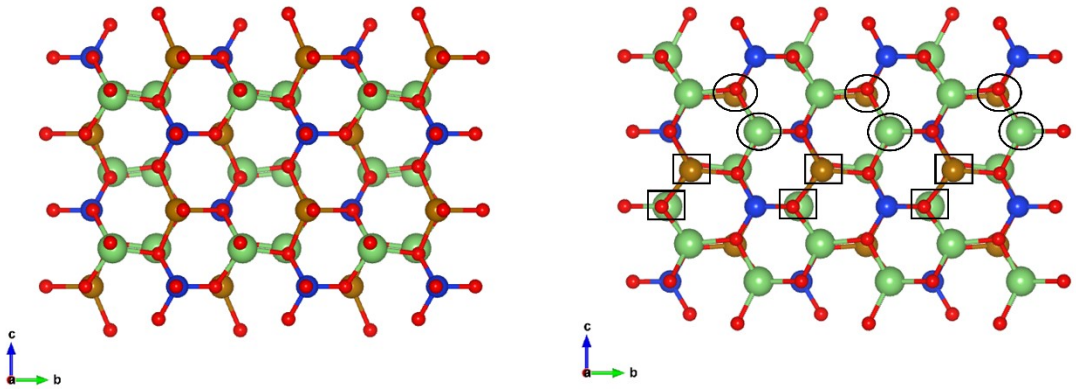

Figure S3 Crystal structures of $Pmn2_1$ Li_2FeSiO_4 (left) and inverse $Pmn2_1$ Li_2FeSiO_4 (right). Fe and Li in rectangular boxes and circle boxes exchange their sites, respectively.

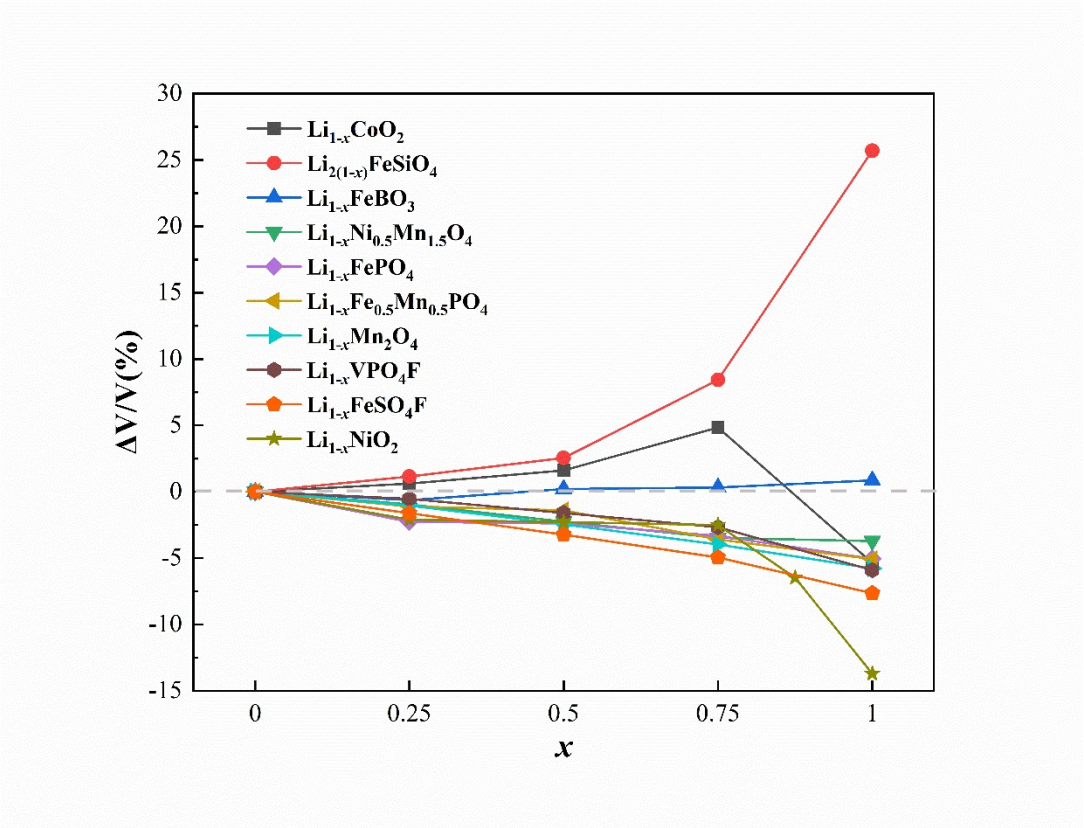

Figure S4 Complete first principles calculated volume change rates of representative intercalation cathodes during delithiation. The *x* here refers to the ratio of the Li^+ deintercalated.

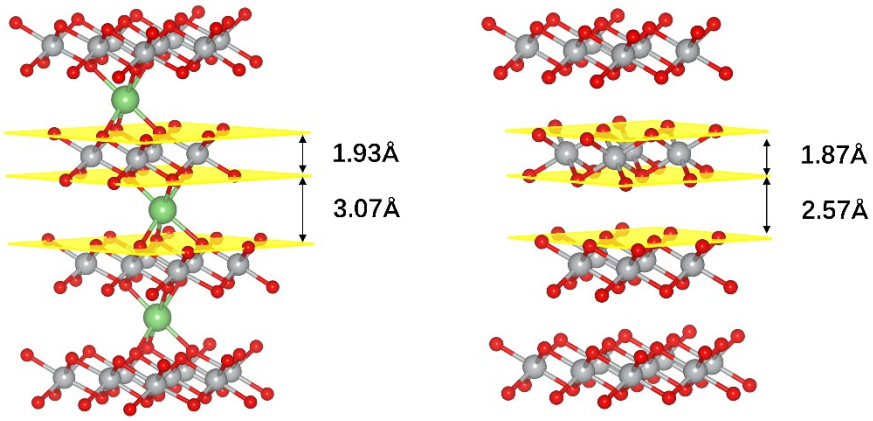

Figure S5 Interlayer(O-Li-O) and intralayer(O-Ni-O) distance of $Li_{0.25}NO_2$ and NiO_2. Grey balls denote Ni ions, while the green and small red ones denote Li ions and oxygen ions.

Table S1 Lattice parameters and formation energy for models of controversial or coexistent structures.

Sample	Structure	*a* (Å)	*b* (Å)	*c* (Å)	*V* (Å^3)	$E\ (eV\,f.u.^{-1})$
$LiNiO_2$	Exp.	2.87	2.87	14.21	101.61	
	$R\bar{3}m$	2.8797	2.8797	14.3495	103.0520	-119.573
	$P2_1/c$	2.8838	2.8837	14.2709	102.7773	-119.944
NiO_2	Exp.	2.81	2.81	13.04	89.45	
	O3	2.7649	2.7649	15.1057	100.0053	-14.185
	O1	2.7708	2.7708	13.3730	88.9145	-14.176
Li_2FeSiO_4	Exp.	6.27	5.33	5.02	167.50	
	$Pmn2_1$	6.3303	5.3831	4.9944	170.1928	-52.898
	β–$Pmn2_1$	6.2598	5.4857	5.0167	172.2634	-53.022
$LiFeBO_3$	Exp.	5.16	9.00	10.41	483.17	
	C2/c	5.1768	9.1087	10.3407	487.3743	-41.425
	C2/c(½00)00	5.2097	8.9907	10.3217	483.2825	-41.602

Table S2. Calculated lattice parameters and volume changes of all the cathode materials investigated in this work. The available previous experimental and DFT calculational values are supplied (previous DFT calculational values in parentheses).

Sample	**Structure**	***a_cal.*** **(Å)**	***a_exp.*** **(Å)**	***b_cal.*** **(Å)**	***b_exp.*** **(Å)**	***c_cal.*** **(Å)**	***c_exp.*** **(Å)**	***V_cal.*** **(Å^3)**	***V_exp.*** **(Å^3)**	***ΔV/V_cal.***	***ΔV/V_exp.***
$LiCoO_2$	$R\bar{3}m$/O3	2.8301 (2.93)[7]	2.82[8]	2.8301	2.82	14.1301 (13.2)	14.06	98.0132 (98.13)	96.61		
$Li_{0.75}CoO_2$		2.8225		2.8193		14.3049		98.6153		0.614%	
$Li_{0.5}CoO_2$	M	2.8033	2.81[9]	2.8297	2.81	14.5457	14.42	99.5901	98.45	1.609%	1.868%
$Li_{0.25}CoO_2$		2.8124		2.8165		14.9829		102.7538		4.837%	
CoO_2	P3m1/O1	2.8338 (2.88)[7]	2.82[8]	2.8336	2.82	13.3355 (12.26)	12.88	92.7484 (88.08)	88.82	-5.372%	-8.063%
$LiNiO_2$	$P2_1/c$	5.6977[a] (4.98)[10]	2.87[11]	2.9178 (2.93)	2.87	14.2745 (14.73)	14.21	101.8743 (102.672)	101.61		
$Li_{0.75}NiO_2$	$R\bar{3}m$	2.8508		2.8508		14.33375		100.8843		-2.103%	
$Li_{0.5}NiO_2$	C2/m	5.6292	4.94[11]	2.8328	2.82	4.8757	5.09	100.6926	100.30	-2.290%	-1.292%

Sample	**Structure**	***a_cal.* (Å)**	***a_exp.* (Å)**	***b_cal.* (Å)**	***b_exp.* (Å)**	***c_cal.* (Å)**	***c_exp.* (Å)**	***V_cal.* (Å^3)**	***V_exp.* (Å^3)**	***ΔV/V_cal.***	***ΔV/V_exp.***
$Li_{0.25}NiO_2$	$R\bar{3}m$	2.7849	2.82[11]	2.8077	2.82	14.9151	14.39	100.4631	98.87	-2.512%	-2.699%
$Li_{1/9}NiO_2$	$R\bar{3}m$	2.7735		2.7832		14.4334		96.37254		-6.482%	
NiO_2	P3m1 / O1	2.7708 (2.87)[7]	2.81[12]	2.7708	2.81	13.3730 (11.72)	13.04	88.9145 (83.61)	89.45	-13.719%	-11.970%
$LiMn_2O_4$	$Fd\bar{3}m$	8.2979 (8.25)[13]	8.24[14]	8.3259	8.24	8.5387	8.24	589.8782	559.92		
$Li_{0.75}Mn_2O_4$	$Fd\bar{3}m$	8.2873		8.3453		8.4415		583.7131		-1.045%	
$Li_{0.5}Mn_2O_4$	$Fd\bar{3}m$	8.2812 (8.32)[13]	8.15[14]	8.4904	8.15	8.1853	8.15	575.3687	541.43	-2.460%	-3.304%
$Li_{0.25}Mn_2O_4$	$Fd\bar{3}m$	8.2409		8.3762		8.2089		566.4769		-3.967%	
MnO_2	$Fd\bar{3}m$/ λ - MnO_2	8.2260 (8.40)[13]	8.06[15]	8.2260	8.06	8.2260	8.06	556.6251	524.44	-5.779%	-6.337%
$LiNi_{0.5}Mn_{1.5}O_4$	$P4_332$	8.2694 (8.290)[16]	8.17[17]	8.2693	8.17	8.2692	8.17	565.4633	544.74		

Sample	**Structure**	***a_cal.*** **(Å)**	***a_exp.*** **(Å)**	***b_cal.*** **(Å)**	***b_exp.*** **(Å)**	***c_cal.*** **(Å)**	***c_exp.*** **(Å)**	***V_cal.*** **(Å^3)**	***V_exp.*** **(Å^3)**	***ΔV/V_cal.***	***ΔV/V_exp.***
$Li_{0.75}Ni_{0.5}Mn_{1.5}O_4$	$P4_332$	8.2095		8.2079		8.3122		560.0840		-0.951%	
$Li_{0.5}Ni_{0.5}Mn_{1.5}O_4$	$P4_332$	8.2330	8.09[17]	8.1931	8.09	8.1943	8.09	552.7209	529.87	-2.253%	-2.730%
$Li_{0.25}Ni_{0.5}Mn_{1.5}O_4$	$P4_332$	8.2351		8.1381		8.1442		545.8031		-3.477%	
$Ni_{0.5}Mn_{1.5}O_4$	$P4_332$	8.1797	8.01[17]	8.1589	8.01	8.1590	8.01	544.4117	512.96	-3.723%	-5.834%
$LiFePO_4$	Pnma	4.7424 (4.67)[18]	4.69[19]	6.0617 (5.96)	6.01	10.4238 (10.22)	10.33	299.6498	291.20		
$Li_{0.75}FePO_4$	Pnma	4.7908		6.0127		10.3153		297.1060		-0.849%	
$Li_{0.5}FePO_4$	Pnma	4.8026		5.9842		10.1710		292.3120		-2.449%	
$Li_{0.25}FePO_4$	Pnma	4.8431		5.9417		10.0684		289.6799		-3.327%	
$FePO_4$	Pnma	4.8613 (4.81)[18]	4.78[19]	5.8900 (5.89)	5.79	9.9358 (9.97)	9.81	284.4901	271.50	-5.059%	-6.765%

Sample	**Structure**	***a_cal.* (Å)**	***a_exp.* (Å)**	***b_cal.* (Å)**	***b_exp.* (Å)**	***c_cal.* (Å)**	***c_exp.* (Å)**	***V_cal.* (Å^3)**	***V_exp.* (Å^3)**	***ΔV/V_cal.***	***ΔV/V_exp.***
$LiFe_{0.5}Mn_{0.5}PO_4$	Pnma	4.7648 (4.681)[20]	4.771[21]	6.1095 (5.978)	6.106	5.2511 (5.13)	5.25	305.7246			
$Li_{0.75}Fe_{0.5}Mn_{0.5}PO_4$	Pnma	4.8064		6.0812		10.3443		302.3278		-1.111%	
$Li_{0.5}Fe_{0.5}Mn_{0.5}PO_4$	Pnma	4.8595		6.0297		5.1447		301.4339		-1.403%	
$Li_{0.25}Fe_{0.5}Mn_{0.5}PO_4$	Pnma	4.8836		6.0062		10.0494		294.7496		-3.590%	
$Fe_{0.5}Mn_{0.5}PO_4$	Pnma	4.8993		5.9822		4.9514		290.2083		-5.075%	
$LiFeSO_4F$	$P\bar{1}$	5.2193 (5.23)[22]	5.17[4]	5.5706 (5.59)	5.49	7.3859 (7.42)	7.22	190.5452	182.56		
$Li_{0.75}FeSO_4F$	$P\bar{1}$	5.1747		5.5087		7.4325		187.4742		-1.612%	
$Li_{0.5}FeSO_4F$	$P\bar{1}$	5.2414		5.3903		7.3950		184.3951		-3.228%	
$Li_{0.25}FeSO_4F$	$P\bar{1}$	5.2579		5.2941		7.3801		181.1117		-4.951%	

Sample	**Structure**	***a_cal.*** **(Å)**	***a_exp.*** **(Å)**	***b_cal.*** **(Å)**	***b_exp.*** **(Å)**	***c_cal.*** **(Å)**	***c_exp.*** **(Å)**	***V_cal.*** **(Å^3)**	***V_exp.*** **(Å^3)**	***ΔV/V_cal.***	***ΔV/V_exp.***
$FeSO_4F$	$P\bar{1}$	5.2100 (5.20)[22]	5.07[4]	5.2376 (5.22)	5.08	7.3420 (7.36)	7.34	175.9528	163.64	-7.658%	-10.363%
$LiVPO_4F$	$P\bar{1}$	5.2310 (5.20)[23]	5.17[5]	5.3813 (5.35)	5.31	7.4158 (7.39)	7.26	182.9564	174.36		
$Li_{0.75}VPO_4F$	$P\bar{1}$	5.2163		5.3594		7.4432		181.9756		-0.536%	
$Li_{0.5}VPO_4F$	$P\bar{1}$	5.2578		5.2703		7.4459		180.0181		-1.606%	
$Li_{0.25}VPO_4F$	$P\bar{1}$	5.2393		5.2498		7.4259		178.0739		-2.669%	
VPO_4F	C2/c	7.4130	7.16[5]	7.2068	7.13	7.4971	7.35	172.1571	160.50	-5.903%	-7.949%
Li_2FeSiO_4	β-$Pmn2_1$	6.2598 (6.2675)[24]	6.27[25]	5.4857 (5.4928)	5.33	5.0167 (5.0228)	5.02	172.2634	167.50		
$Li_{1.5}FeSiO_4$	β-$Pmn2_1$	6.3995		5.4089		5.0347		174.2395		1.147%	
$LiFeSiO_4$	β-$Pmn2_1$	6.6997 (6.6996)[24]	6.51[25]	5.2026 (5.2295)	5.22	5.0678 (5.0813)	5.00	176.6408	169.80	2.541%	1.373%

Sample	**Structure**	***a_cal.*** **(Å)**	***a_exp.*** **(Å)**	***b_cal.*** **(Å)**	***b_exp.*** **(Å)**	***c_cal.*** **(Å)**	***c_exp.*** **(Å)**	***V_cal.*** **(Å^3)**	***V_exp.*** **(Å^3)**	***ΔV/V_cal.***	***ΔV/V_exp.***
$Li_{0.5}FeSiO_4$	β-$Pmn2_1$	7.0067		5.2118		5.1166		186.7870		8.431%	
FeSiO4	β-$Pmn2_1$	7.3980 (7.484)[24]		5.4516 (5.417)		5.3690 (5.378)		216.5349		25.700%	
$LiFeBO_3$	C2/c(½00)00	5.2097 5.162[26]	5.17[27]	8.9907 (8.995)	8.87	10.3217 (10.409)	10.16	483.2825	465.78		
$Li_{0.75}FeBO_3$	C2/c(½00)00	5.2310		8.9724		10.2402		480.2254		-0.633%	
$Li_{0.5}FeBO_3$	C2/c(½00)00	5.2015		9.0784		10.2568		484.2849		0.207%	
$Li_{0.25}FeBO_3$	C2/c(½00)00	5.2753		9.0420		10.1649		484.8320		0.321%	
$FeBO_3$	C2/c(½00)00	5.3628 (5.308)[26]		8.9728 (8.989)		10.2162 (10.188)		491.5208		0.851%	<2%[28]

[a] The space group of computational $LiNiO_2$ model is $P2_1/c$, whose parameter a is twice as large as that of $R\bar{3}m$.

Table S3. Shannon radii (in angstrom) of transition metals in different valence states.[29]

Charge	Ni	Co	Mn	Fe	V
+2	0.69		0.83	0.78	
+3	0.56	0.61	0.645	0.645	0.64
+4	0.48	0.53	0.53		0.58

Table S4. Bond lengths and J-T distortion degrees of $LiCoO_2$ and $LiNiO_2$ after different content Li^+ ions are delithiated.

Sample	$L_{M\text{-}O1}$(Å)	$L_{M\text{-}O2}$(Å)	$L_{M\text{-}O3}$(Å)	$L_{M\text{-}O4}$(Å)	$L_{M\text{-}O5}$(Å)	$L_{M\text{-}O6}$(Å)	$L_{average}$[a](Å)	J-T[b](%)
$LiCoO_2$	1.93235	1.93235	1.93233	1.93234	1.93233	1.93235	1.93234	0.001%
$Li_{0.5}CoO_2$	1.89903	1.90094	1.89903	1.89795	1.89873	1.89793	1.89894	0.159%
CoO_2	1.88349	1.88376	1.88363	1.88357	1.88368	1.88356	1.88362	0.014%
$LiNiO_2$	1.90437	1.89822	2.10754	2.09998	1.90036	1.90899	1.96991	10.626%
$Li_{0.75}NiO_2$	1.91669	1.91668	2.08616	2.08616	1.90356	1.90356	1.96880	9.275%
$Li_{0.5}NiO_2$	1.86276	2.01728	2.01702	1.90501	1.88638	1.88935	1.92963	8.008%
$Li_{0.25}NiO_2$	1.86833	1.84815	1.84998	1.8415	1.86864	1.85729	1.85565	1.463%
NiO_2	1.85431	1.85403	1.85387	1.85413	1.85431	1.85403	1.85411	0.024%

[a] arithmetic average bond length of M-O

[b] defined as the difference between the longest and shortest M-O distances divided by the average M-O distance of the MO_6 trigonal bipyramids

Table S5. Calculated crystal parameters *a*, *b*, *c,* and *L-J-T* values of $LiMn_2O_4$ and $LiNi_{0.5}Mn_{1.5}O_4$ after different content Li^+ ions are delithiated.

Sample	*a*(Å)	*b*(Å)	*c*(Å)	*L-J-T*[a](%)
$LiMn_2O_4$	8.298	8.539	8.326	2.87%
$Li_{0.5}Mn_2O_4$	8.281	8.49	8.185	3.67%
Mn_2O_4	8.226	8.226	8.226	0.00%
$LiNi_{0.5}Mn_{1.5}O_4$	8.269	8.269	8.269	0.00%
$Li_{0.5}Ni_{0.5}Mn_{1.5}O_4$	8.233	8.1931	8.194	0.49%
$Ni_{0.5}Mn_{1.5}O_4$	8.18	8.159	8.159	0.26%

[a] *L-J-T* is calculated from the difference between the longest and shortest crystal parameters divided by the average crystal parameter.

Table S6 Calculated magnetic moments (μ_B) of transition metal ions after different content Li^+ ions are delithiated

Charge	Mag. [a](Fe)	Mag. (Mn)	Mag. (Ni)
$Li_8Mn_{16}O_{32}$		3.2×8 3.9×8	
$Li_4Mn_{16}O_{32}$		3.2×12 3.9×4	
$Mn_{16}O_{32}$		3.3×16	
$Li_8Ni_4Mn_{12}O_{32}$		3.2×12	1.8×4
$Li_4Ni_4Mn_{12}O_{32}$		3.2×12	1.3×4

$Ni_4Mn_{12}O_{32}$		3.2×12	0.4×4
$Li_8Fe_4Mn_4(PO_4)_8$	3.8×4	4.7×4	
$Li_4Fe_4Mn_4(PO_4)_8$	4.4×4	4.7×4	
$Fe_4Mn_4(PO_4)_8$	4.4×4	3.9×4	

Table S7. Calculated change rates of P-O and M-O bond length after M ions (M=Fe, Mn) oxidization and volume change rates of $LiFePO_4$ and $LiFe_{0.5}Mn_{0.5}PO_4$ after half-(ΔV%_half) and fully-(ΔV%_all) Li extracted.

Sample	P-O	Fe-O	Mn-O	ΔV%_half	ΔV%_all
$LiFePO_4$	-0.39%	-5.80%		-2.449%	-5.059%
$LiFe_{0.5}Mn_{0.5}PO_4$	-0.39%	-5.47%	-5.90%	-1.403%	-5.075%

Table S8. Change rates of NM-O (NM=P, S) and M-O(F) (M=V, Fe) bond length after M ions oxidization and volume change rates of $LiVPO_4F$ and $LiFeSO_4F$ after half (ΔV%_half) and fully (ΔV%_all) Li extracted.

Sample	NM-O	M-O(F)[a]	ΔV%_half	ΔV%_all
$LiVPO_4F$	-0.34%	-4.58%	-1.606%	-5.903%
$LiFeSO_4F$	-0.48%	-7.15%	-2.666%	-7.658%

[a] bond length of M-O(F) is the weighted average of four M-O and two M-F bonds

Table S9. Change rates of NM-O (NM=Si, B) and Fe-O bond length after Fe^{2+} ions oxidized to Fe^{3+} and volume change rates of Li_2FeSiO_4 and $LiFeBO_3$ after Li^+ half (ΔV%_half) and fully (ΔV%_all) extracted.

Sample	NM-O	Fe-O	ΔV%_half	ΔV%_all
Li_2FeSiO_4	-0.57%	-6.81%	2.54%	25.70%
$LiFeBO_3$	-0.76%	-7.29%	0.21%	0.85%

REFERENCES

1. M. Bianchini, M. Roca-Ayats, P. Hartmann, T. Brezesinski and J. Janek, *Angew. Chem. Int. Ed.*, 2019, **58**, 10434-10458.
2. A. Rougier, P. Gravereau and C. Delmas, *J. Electrochem. Soc.*, 1996, **143**, 1168-1175.
3. S.-H. Bo, F. Wang, Y. Janssen, D. Zeng, K.-W. Nam, W. Xu, L.-S. Du, J. Graetz, X.-Q. Yang, Y. Zhu, J. B. Parise, C. P. Grey and P. G. Khalifah, *J. Mater. Chem.*, 2012, **22**.
4. N. Recham, J. N. Chotard, L. Dupont, C. Delacourt, W. Walker, M. Armand and J. M. Tarascon, *Nat. Mater.*, 2010, **9**, 68-74.
5. J.-M. A. Mba, L. Croguennec, N. I. Basir, J. Barker and C. Masquelier, *J. Electrochem. Soc.*, 2012, **159**, A1171-A1175.
6. R. Malik, A. Abdellahi and G. Ceder, *J. Electrochem. Soc.*, 2013, **160**, A3179-A3197.
7. M. K. Aydinol, A. F. Kohan, G. Ceder, K. Cho and J. Joannopoulos, *Phys. Rev. B*, 1997, **56**, 1354-1365.
8. G. G. Amatucci, J. M. Tarascon and L. C. Klein, *J. Electrochem. Soc.*, 1996, **143**, 1114-1123.
9. J. N. Reimers and J. R. Dahn, *J. Electrochem. Soc.*, 1992, **139**, 2091-2097.
10. H. Das, A. Urban, W. Huang and G. Ceder, *Chem. Mater.*, 2017, **29**, 7840-7851.
11. H. Li, N. Zhang, J. Li and J. R. Dahn, *J. Electrochem. Soc.*, 2018, **165**, A2985-A2993.
12. L. Croguennec, *Solid State Ionics*, 2000, **135**, 259-266.
13. B. Xu and S. Meng, *J. Power Sources*, 2010, **195**, 4971-4976.

14. K. Kanamura, H. Naito, T. Yao and Z. I. Takehara, *J. Mater. Chem.*, 1996, **6**, 33-36.

15. J. O. T. Berg. H, *Solid State Ionics*, 1999, **126**, 227-234.

16. X.-G. Xin, J.-Q. Shen and S.-Q. Shi, *Chinese Physics B*, 2012, **21**, 128202.

17. K. Ariyoshi, Y. Iwakoshi, N. Nakayama and T. Ohzuku, *J. Electrochem. Soc.*, 2004, **151**, A296.

18. J. Jiang, C. Ouyang, H. Li, Z. Wang, X. Huang and L. Chen, *Solid State Commun.*, 2007, **143**, 144-148.

19. W. J. Zhang, *J. Power Sources*, 2011, **196**, 2962-2970.

20. A. K. Budumuru, M. Viji, A. Jena, B. R. K. Nanda and C. Sudakar, *J. Power Sources*, 2018, **406**, 50-62.

21. W. Huang, S. Tao, J. Zhou, C. Si, X. Chen, W. Huang, C. Jin, W. Chu, L. Song and Z. Wu, *The Journal of Physical Chemistry C*, 2014, **118**, 796-803.

22. Z. Liu and X. Huang, *Solid State Ionics*, 2010, **181**, 1209-1213.

23. F. Jiang, Y. Di, E. Liu, S. Chen, F. Chen, X. Zhu, X. Wang, Z. Lu and D. Huang, *J. Solid State Electrochem.*, 2020, **24**, 1075-1084.

24. J. Yang, J. Zheng, X. Kang, G. Teng, L. Hu, R. Tan, K. Wang, X. Song, M. Xu, S. Mu and F. Pan, *Nano Energy*, 2016, **20**, 117-125.

25. A. Nytén, S. Kamali, L. Häggström, T. Gustafsson and J. O. Thomas, *J. Mater. Chem.*, 2006, **16**, 2266-2272.

26. S. Loftager, J. M. García-Lastra and T. Vegge, *The Journal of Physical Chemistry C*, 2016, **120**, 18355-18364.

27. Y. Janssen, D. S. Middlemiss, S. H. Bo, C. P. Grey and P. G. Khalifah, *J. Am. Chem. Soc.*, 2012, **134**, 12516-12527.

28. A. Yamada, N. Iwane, Y. Harada, S. Nishimura, Y. Koyama and I. Tanaka, *Adv. Mater.*, 2010, **22**, 3583-3587.

29. R. D. Shannon, *Acta Crystallographica*, 1976, **32**, 751-767.